FEM-based thermal analysis of NiMH batteries for hybrid vehicles

W. Renhart C. Magele and B. Schweighofer

***Abstract*— Hybrid vehicles require advanced battery management systems. Amongst others the knowledge of the temperature during operation is substantially. This parameter strongly affects the behavior of the electrical energy source. In this paper the finite element analysis has been applied to predict the thermal performance capability. Our investigations have been accomplished on a standard NiMH type. The temperature found will be involved in an equivalent battery circuit network in order to simulate realistic drive cycles.**

***Keywords*—Finite elements, NiMH battery, thermal model**

I. Introduction

A special attention in the use of batteries for hybrid vehicles has been focussed on NiMH types. Compared to lead batteries the NiMH cells show a seriously higher specific energy, a better specific power and a longer product life-time. Lithium batteries can be easily over-charged and therefore, give reasons for safety objections. Employing NiCd batteries the toxic cadmium must be handled.

The usage of NiMH batteries necessitates a highly developed battery management system with the temperature as one main control variable. A thermal runaway of the NiMH cells should be avoided. Further goals may be the optimization of charging and discharging cycles as well as the control of overloading effects. Battery management systems must operate in real time. So, the underlying battery models must be designed in a simple way in order to become fast. Unluckily, the various parameters to prescribe the batteries enforce a complex model and we have to find a compromise.

A major aim is the representation of the battery voltage U_B which depends on the temperature, on the state of charge (SOC) and on the instantaneous current extraction over a wide range of operation.

First of all, a very accurate knowledge of the temperature behavior of U_B is necessary. Depending on the electrical current charging or discharging the battery, the electrical power losses within the cell must be determined. In a first step a FEM-computation to get more insight into the current flow field will be applied. Knowing the electrical losses, the internal thermal sources are known, as well. Now, the finite element method can be applied in order to solve the thermal problem. Once the thermal balance has been found, an existing equivalent network model will be extended to include the thermal dependencies. Our model used (Fig. 1) is taken from [1].

Manuscript received June 22, 2007

W. Renhart and C. Magele are with the Institute for Fundamentals and Theory in Electrical Engineering (IGTE); B. Schweighofer is with the Institute of Electrical Measurement and Measurement Signal Processing, all of the Graz University of Technology, Kopernikusgasse 24, A-8010 Graz, Austria. e-mail: werner.renhart@tugraz.at

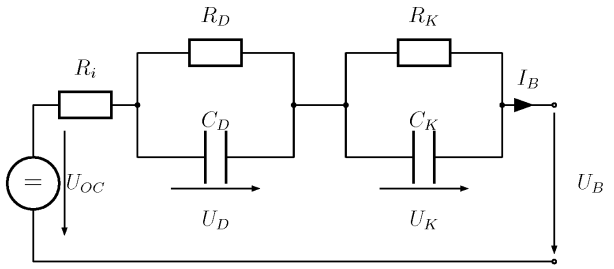

Fig. 1. Equivalent circuit network for the NiMH cell in use.

U_B and I_B represent the terminal voltage and current. The internal resistor R_i takes the electrolyte, the electrodes and the connectors into account. R_D and C_D consider the double layer capacity effects on the surfaces of the electrode whereas the diffusion phenomenons in the electrolyte will be modeled with the elements R_K and C_K. Both RC-elements affect on the transient behavior.

$$\begin{aligned} U_{OC} - (R_i\, I_B + U_D + U_K + U_B) &= 0 \\ \frac{U_D}{R_D} + C_D \frac{d\,U_D}{d\,t} &= I_B \\ \frac{U_K}{R_K} + C_K \frac{d\,U_K}{d\,t} &= I_B \end{aligned} \qquad (1)$$

U_{OC} represents the open circuit voltage. For constant temperature and constant SOC, the network parameters can be found as described in [1]

II. Model formulation

A. SOC-dependance in the model

One main characteristic is the dependency of the battery voltage U_B on the SOC. The nonlinear behavior also is influenced by the magnitude of the current during charging and discharging, respectively.

It is very common to specify the current in terms of the nominal capacity of the battery per hour. So, a current of $4.5A$ charging a $9Ah$ battery is called a $0.5C$ - load. In Fig. 2 the characteristics for loads of $1C$ and of $22.22C$ at a temperature of 20 degree Celsius are given. The sparcely given values for $1C$ and for $22.2C$ taken from

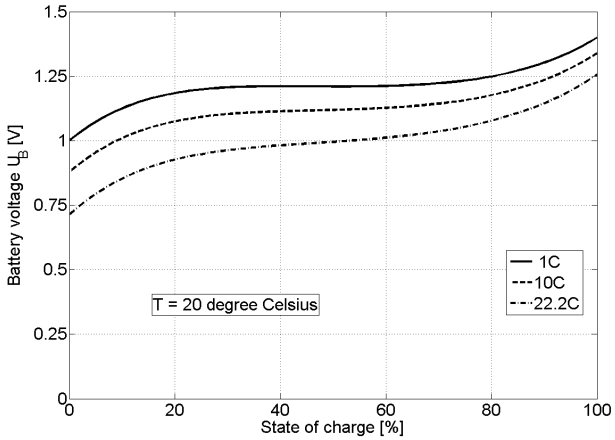

Fig. 2. U_B versus SOC for variant loads, T=constant.

the battery data sheet have been fitted to a curve, subsequently. Hereafter, all further loads, eg. $10C$, will be interpolated linearly.

B. Temperature dependance in the model

Converse to an increasing internal temperature a decrease in kinetic and mass transfer is implicated. The internal ohmic resistance becomes smaller and consequently, the inner power losses drop down. This results in a higher battery voltage U_B at a changeless SOC. Again, the few available data from the battery specification allow, after fitting to a curve, a quantitative description of the temperature influence ([2]).

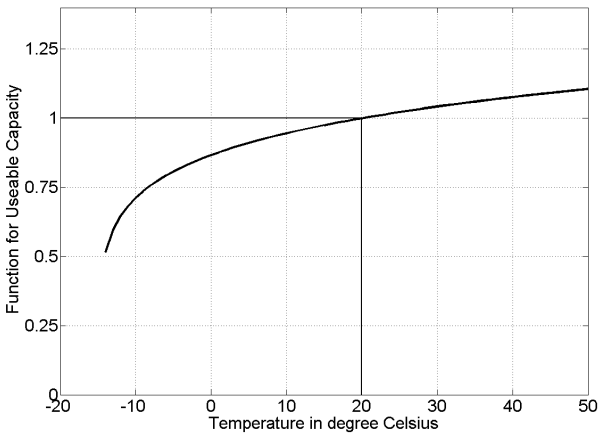

Fig. 3. Correction function for the influence of T on U_B.

Fig. 3 shows the correction function between the temperature range from -15 to $+50$ centigrade. The correction function has been fitted, so that at an internal temperature of $T = 20°C$ no correction has to be accomplished.

C. Finite element thermal model

For solving the thermal problem, the heat conduction equation (2) must be solved [3].

$$\frac{\partial}{\partial x}k_x\frac{\partial T}{\partial x} + \frac{\partial}{\partial y}k_y\frac{\partial T}{\partial y} + \frac{\partial}{\partial z}k_z\frac{\partial T}{\partial z} + \dot{q} = \rho \cdot c\frac{\partial T}{\partial t}. \quad (2)$$

ρ represents the mass density $[kg/m^3]$, c denotes the specific heat capacity $[J/(kg\,K)]$, k_x, k_y, k_z are the thermal conductivity coefficients $[W/(m\,K)]$ in the appropriate direction. $\dot{q}$ stands for the rate of heat generation per unit volume $[W/m^3]$.

A possible heat transfer by convection normal to boundary surfaces to ambience will be modeled with the boundary condition

$$k\frac{\partial T}{\partial n} = h\,(T - T_a). \quad (3)$$

Therein, h is a known heat transfer coefficient $[W/m^2\,K]$, T_a represents the ambient temperature, k again is the thermal conductivity and n denotes the normal direction on the boundary. With this boundary condition, cooling effects may be modeled, as well.

D. Finite element current flow model

In order to find the heat sources in the battery, a FEM-computation for static current flow field problems has to be performed. The standard FEM-formulation uses the electric scalar potential V. With the electric conductivity γ, the electric field vector $\vec{E}$ and the current density vector $\vec{J}$ the governing equations follow:

$$\begin{aligned} \vec{E} = -\nabla V, \qquad \vec{J} &= \gamma\,\vec{E} \\ \nabla\cdot(\gamma\,\nabla V) &= 0. \end{aligned} \quad (4)$$

The outcome of the electric flow computation is the distribution of the power losses and the up to date heat sources for (2) follow:

$$\dot{q} = \frac{P_{loss}}{V_C}, \quad (5)$$

with V_C the volume of the cell. Equation (5) represents the Joule losses inside the cell. Possible losses generated due to electrochemical processes, based on hydrogen absorbing and desorbing reactions will not be included in this model.

III. Simulation procedure

The whole procedure for the simulations is shown in Fig. 4. A fully charged battery (SOC_0= 100%) at a known temperature T_0 build the initial conditions for the simulation procedure. The known charge- and/or discharge cycle for the battery current I_B will be discretized in time. For each time step the actual SOC can be computed precisely. Therewith the up to date battery voltage

U_B, depending on SOC and on the temperature T will be computed applying the previously prescribed SOC- and the temperature model. A proper U_B allows in consequence the computation of the FEM-based current flow field. Hereafter the power losses P_{loss} can be computed and the heat sources are known when evaluating (5). Continued, the thermal FEM-procedure will be applied to obtain the up to date temperature T and the next time step computation can be treated.

After the current flow analysis has been performed the internal ohmic resistance as a function of SOC and of T is known and can be used in the proposed network model (cf. Fig. 1).

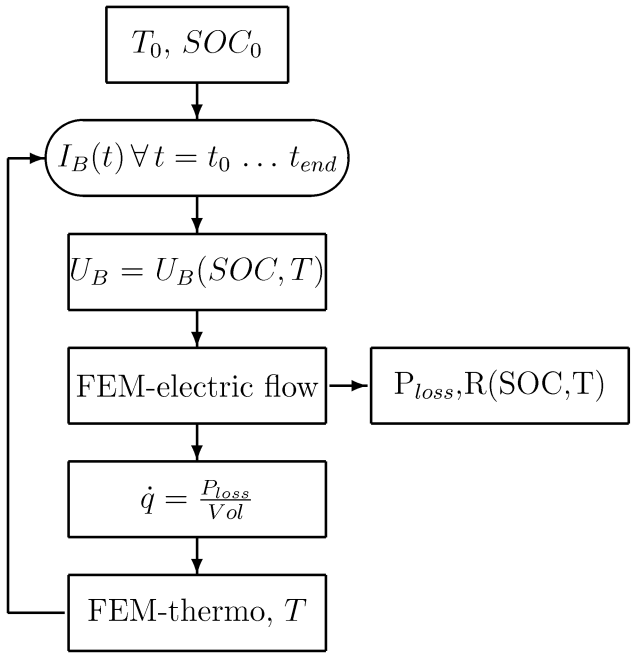

Fig. 4. Flow diagram for the computation procedure.

IV. Finite Element Model of the NiMH cell

A part of the finite element structure of the battery investigated is shown in Fig. 5. It is a NiMH cell, type NR 10 UHP - VARTA with a nominal voltage of 1.3 V and a nominal capacity of 9 Ah.

The battery is assembled in bipolar technique. Thereby, the variant materials alternate in the order: MH - electrode, polyamide separator with electrolyte, Ni - electrode, polyamide separator with electrolyte, MH - electrode and so on. All together are 9 MH - layers inside. For the thermal computations, the thermal capacitance values are taken from [4].

V. Numerical results

The red line in Fig. 6 shows the battery current during the discharging cycles. A constant current extraction of

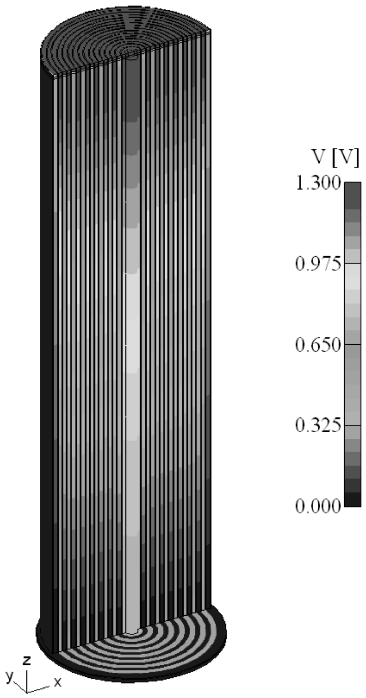

Fig. 5. Potential distribution, part of the structure.

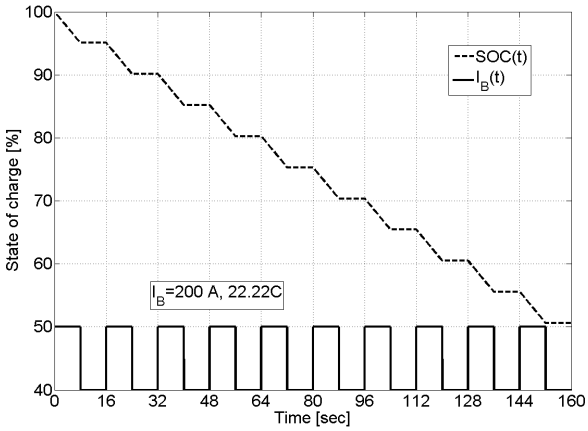

Fig. 6. Current extraction and SOC .

$I_B = 200\,A$ from the battery over 8 seconds alters with 8 seconds of zero current flow. Initially, the battery was charged to the nominal capacity at an ambient temperature of $T = 20°C$. During each discharging phase the SOC decreases linearly in time, whereas no current extraction upholds the SOC reduction, apparent as blue line in Fig. 6. This correlates to a five per cent decay of the nominal SOC at each discharging cycle. After ten cycles the nominal battery capacity is halved. As a result of the thermal FEM-computations, the temperature increase during the cycles is known. Its behavior is plotted in Fig. 7. In case of no energy exchange between battery

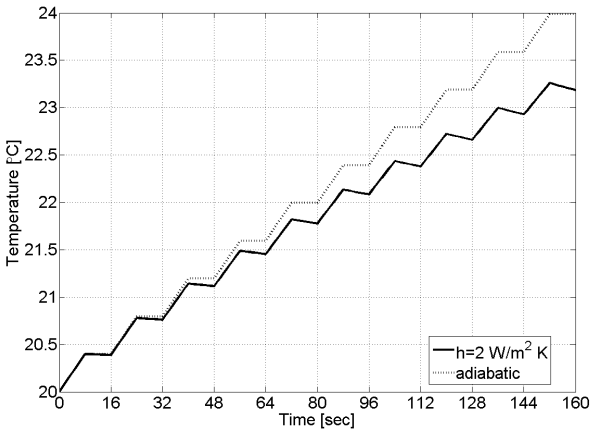

Fig. 7. FEM-computed temperature lapse.

and ambient the utmost temperature increase will be observed. The temperature run for the so called adiabatic process is visualized by the blue line in Fig. 8. The red line shows the behavior in case a heat transfer at the top surface of the battery is allowed. Therefore a coefficient of $h = 2\,W/m^2\,K$ is accounted in the FEM-model when applying (3). During the zero current phases, the system tends to chill to the ambient temperature.

In order to illustrate the influence of the temperature T on the the battery voltage, U_B is plotted in Fig. 8. The blue line corresponds to the solution when the proposed temperature model is considered. The red line takes the actual SOC without any thermal influence into account.

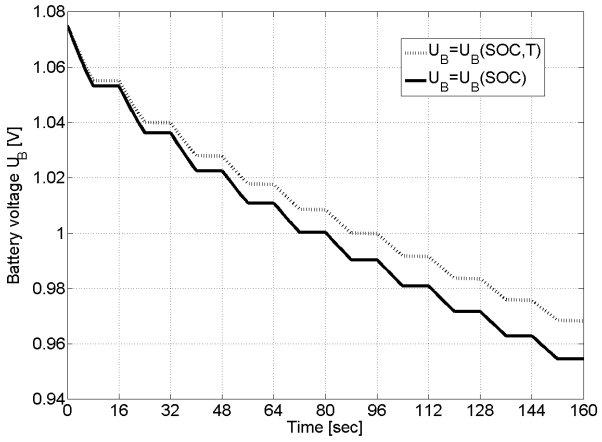

Fig. 8. Run of battery voltage in comparison.

To valuate the proposed models, some comparison between simulated solutions and measurements have been carried out. Corresponding to the battery current cycles shown in Fig. 6, the battery terminal voltage U_B has been measured and is represented by the blue solid line in Fig. 9. A temperature rise from $20°\,C$ at the beginning up to $24.1°\,C$ at the end of the cycles has been observed. Paying regard to the temperature curves shown in Fig. 7 the temperature measured is very close to the adiabatic characteristic.

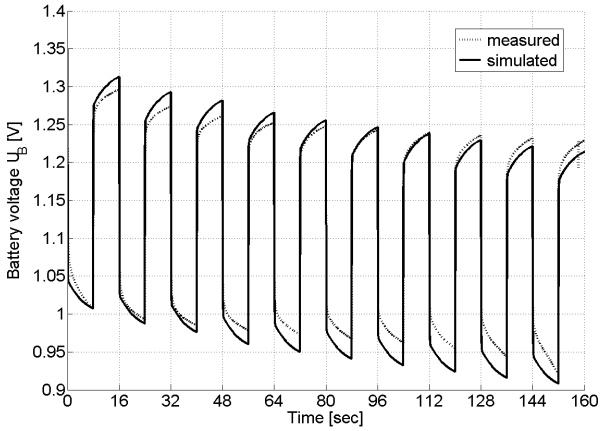

Fig. 9. Measured and network simulated results.

Consequently, the FEM-computed temperature is a bit to low in the model. This behavior appears in the deviation to the simulated battery voltage in Fig. 9, as well. A higher temperature leads to a higher $U_B(SOC, T)$ by reason of the increase of the correction function (Fig. 3).

VI. Conclusion

A FEM-supported way to extend a widely used battery network model in order to consider thermal influences has been proposed. Therefore, a possibility to model the dependance of the battery voltage from the SOC, from the battery current and from the temperature has been shown. The application of a thermal FEM-code enables the actual temperature of the battery during runtime to be known.

Finding appropriate parameters from data sheets to model the variant influences is a major difficulty, thereby. Several effects like self discharge and hysteresis between charging and discharging process are not yet implemented in the model. Especially, the later effect may become important at large current extraction. An adaptation of the suggested procedure for different battery types will be subject for continuative investigations.

References

[1] B. Schweighofer, K.M. Raab, G. Brasseur, "Modeling of High Power Automotive Batteries by the Use of Automated Test Systems", *IEEE Instr. and Meas.*, Vol. 52, No. 4, August 2003, pp. 1087-1091.

[2] M. Chen, G.A.Rincon-Mora, "Accurate Electrical Battery Nodel Capable of Predicting Runtime and I-V Performance", *IEEE Trans. on Energy Conversion*, Vol. 21, No. 2, June 2006, pp. 504-511.

[3] M.N. Özisik, "Heat Transfer - A Basic Approach", *McGrawHill*, 1985, chapter 2.

[4] C.Y. Wang, W.B. Gu, "Thermal-Electrochemical Modeling of Battery Systems", *J. Electrochemistry*, Vol. 147, 2000, p. A2910.